Fizika Nizkikh Temperatur, 1996, v. 22, No 2, p. 134–139

High resolution infrared spectroscopy of $Q_1(0)$ transitions in parahydrogen crystals induced by laser radiation field, external electric field, impurity quadrupole field, and the Coulomb field of charges

Takeshi Oka

Department of Chemistry and Department of Astronomy and Astrophysics, Enrico Fermi Institute
University of Chicago, Chicago, IL 60637, USA
E-mail:oka@biovax.uchicago.edu

1. Introduction

Let me start by reminding you of the two beautiful characteristics of the para-H_2 crystal as a specimen for high resolution spectroscopy.

1.1. Quantum crystal

Solid hydrogen is a weakly bound system. The H_2–H_2 dispersion interaction has the equilibrium binding energy of $D_e \approx 25\ \mathrm{cm}^{-1}$ [1], but after subtracting the zeropoint energy, the energy of stabilization is only $D_0 \approx 2.9\ \mathrm{cm}^{-1}$ [2]. This weakness of the binding together with the small mass of H_2 makes solid hydrogen (together with solid He) a special category of crystals which Lou Nosanow christened with the name of «Quantum Crystals» [3]. For such crystals «the root-mean-square deviation of a particle from its lattice site is not small compared to the nearest-neighbor distance. The problem is not simply that the anharmonic terms are large; it is that the harmonic approximation itself breaks down» [3]. Moreover, the constituents of a quantum crystal may exchange their positions due to quantum mechanical tunneling effect. This is well established for solid ^{3}He from spin resonance experiments and observation of phase transitions in the mK region, in which the exchange was shown to occur with the time scale of microseconds [4,5]. This type of exchange is expected also in solid hydrogen [6] although its frequency is likely to be lower than in He because of a higher binding energy ($D_e \approx 25\ \mathrm{cm}^{-1}$ versus $7.1\ \mathrm{cm}^{-1}$ for He). Theoretical estimates of the exchange time of 10^4–10 sec [7] and 10^{-4} sec [8] have been given. It will be awfully nice if this effect is observed experimentally. In any case this tunneling, even after the formation of crystals, makes solid hydrogen *self-repairing*. This agrees with our experience; nature helps us making nice crystals in spite of our clumsiness and the crystal keeps its order after harsh γ-ray irradiation.

1.2. Singly occupied quantum state

Because of the weak intermolecular interaction, which keeps the molecules at the intermolecular distance of 3.793 Å, and because of the high symmetry of the crystal, and the nearly spherical charge distribution in the hydrogen molecule, the motion of constituent molecules are well quantized. Unlike in other molecular crystals, the rotational quantum number J may be regarded as a good quantum number. The unique aspect of the para-H_2 crystal as a spectroscopic specimen is that all molecules in the crystal occupy the single lowest state at He temperature. This is the state in which all quantum numbers are zero; not only the quantum numbers associated with motion such as the electronic orbital angular momentum L, the vibrational quantum number v, and the rotational quantum number J, but also the total electron and nuclear spin quantum numbers S and I are zero due to the principle of superposition and the Pauli principle. All molecules with the number density of $2.61 \cdot 10^{22}\ \mathrm{cm}^{-3}$, except for the $J = 1$ ortho-H_2 impurity ($\gtrsim 0.06\%$) and HD ($\sim 0.03\%$) in natural abundance, are in the identical quantum state ready to interact with radiation. Such a uniform crystal state has quantum mechanical translational symmetry in addition to the point group symmetry of D_{3h}. This symmetry leads to the momentum quantum number k which is also zero in the ground state but may take any of the N values in the first Brillouin zone if a molecular quantum state is excited [9]. It is the selection rule $\Delta k = 0$ that plays a major role in the discussion of this talk.

2. Pure vibrational $Q_1(0)$ transitions [10,11]

The pure vibrational transition $Q_1(0)$, in which the vibrational state of H_2 is excited ($v = 1 \leftarrow 0$) but the rotational state remains in the lowest state ($J = 0 \leftarrow 0$), is dipole forbidden since

$$\langle J = 0 \mid \vec{\mu} \cdot \mathbf{E} \mid J = 0 \rangle = 0,$$

where $\vec{\mu}$ is the dipole moment operator and E is the radiation electric field. It is doubly forbidden for an electric dipole moment through the parity rule and the angular momentum triangle relation. It becomes allowed if there exists an additional field which admixes a small fraction of the electronic excited state with opposite parity and $J = 1$ to the ground state. The transition moment then is given by the well known Kramers—Heisenberg formula

$$\sum_n \frac{\langle 0 \mid \vec{\mu} \cdot \mathbf{E} \mid n \rangle \langle n \mid \vec{\mu} \cdot \mathbf{E}' \mid 0 \rangle}{W_0 - W_n + \hbar\omega},$$

where E' and ω are the additional field and its frequency, and W_0 and W_n are the energies of the ground state and the n-th electronic state, respectively.

In this talk I give four examples of this type of transitions induced in para-H_2 crystals through different electric fields. The effects, the electric fields, and their orders of magnitude are summarized in Table 1.

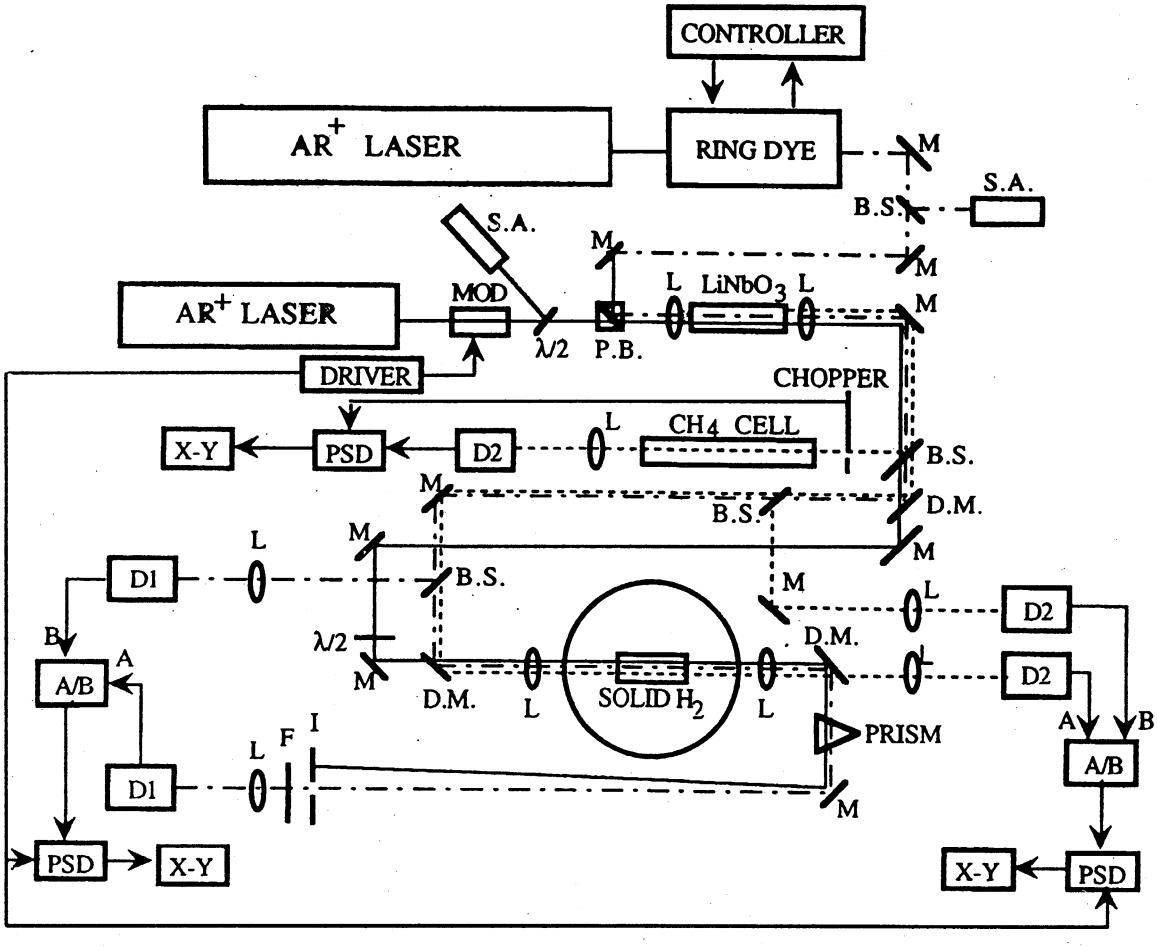

Fig. 1. Block diagram of the Raman/infrared spectrometer used in the observation of the variety of $Q_1(0)$ transition. For the stimulated Raman gain spectroscopy, radiations from a single mode Ar^+ ion laser and the dye laser we used for the pump and probe, respectively. After passing the solid H_2 sample, the two radiations were separated by a prism, and the dye laser radiation was detected. Radiofrequency sidebands were generated on the Ar laser radiation by an electro-optic modulator for the tone-burst modulation. For the infrared spectroscopy, the two visible radiations were mixed in a temperature controlled $LiNbO_3$ crystal to generate infrared radiation. The radiation was passed through the solid H_2 sample and detected by an InSb detector. The technique of the tone-burst modulation was also used for the infrared spectroscopy. If desired, we could record Raman and infrared spectra simulatneously (see Fig. 7). Notations are: M, mirror; L, lens; B.S., beam splitter; S.A., spectrum analyzer; P.B., polarizing beam splitter; Mod, modulator; D.M., dichroic mirror; $\lambda/2$, half wave plate; PSD, phase-sensitive detector; F, filter; D, detector; A/B, differential amplifier; X-Y, XY recorder.

Table 1

No	Effect	Electric field	Order of magnitude, kV/cm
1	Stimulated Raman	Laser radiation field	1
2	Condon	External dc field	10
3	Impurity	Quadrupolar field of $J = 1$ H_2	10^3
4	Ionization	Coulomb field of charges	10^5

While all these four are electric field-induced effects, there are qualitative differences in the observed spectrum and its analysis. In cases 1 and 2 (see Table 1), all molecules more or less feel the same field; the translational symmetry is maintained and the resulting $\Delta k = 0$ rule is well obeyed. In cases 3 and 4, the source of the field is localized on impurity or charge and varies drastically depending on the relative positions of the molecules. The given orders of magnitude for the electric field are those for the nearest neighbor. For the impurity-induced spectrum, the short range $1/R^4$ quadrupolar field destroys the translational symmetry and the $\Delta k = 0$ rule is not followed. On the other hand, for the charge induced spectrum we found, to our surprise, that the $\Delta k = 0$ rule is observed due to the long-range nature of the Coulomb field. The orders of magnitude of the electric field given above for 1 and 2 are those applicable at this stage of development but by no means limited to those values. In particular, for the Condon effect, we should be able to increase the field by an order of magnitude. Since the transition intensity is proportional to the square of the field this should greatly increase the signal. In the following I give the results of our experiment briefly.

3. Stimulated Raman spectrum [12,13]

We used an Ar^+ ion laser at 476.6 nm for the pump and a dye laser at 594.1 nm for the tunable probe radiation. A block diagram of the apparatus is given in Fig. 1. The Ar laser radiation is either amplitude or tone burst modulated and the gain of the probe radiation at resonance is detected. Two examples of observed spectra are given in Fig. 2. When the impurity concentrations are low, the signal is very sharp indicating the remarkable purity of the vibron Bloch states and the rigor of the $\Delta k = 0$ selection rule. When the impurity concentration is increased, the spectrum starts to show structure as shown on the right. The structure is yet to be interpreted.

4. Condon spectrum [14]

After observing the beautiful $\Delta k = 0$ Raman signal, we attempted to observe the variation of its frequency

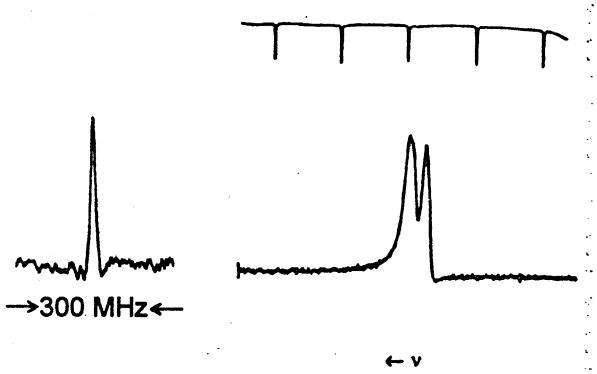

Fig. 2. Stimulated Raman gain spectrum of a para-H_2 crystal. On the left is a sharp spectral line ($\Delta\nu \sim 7$ MHz *hwhm*) for a low ortho-H_2 concentration (0.06%) indicating the purity of the vibron Bloch state and the $\Delta k = 0$ rule. On the right are broader lines for higher ortho-H_2 concentration (2%). The cause of the structure is yet to be understood. The interference markers are separated by 0.05 cm^{-1}.

and lineshape with temperature. This turned out to be not easy; since the accuracy of locating the center of the peak is ~ 1 MHz, we had to stabilize the frequencies of both the Ar laser and the dye laser to a fraction of MHz and measure their frequency individually to the same accuracy. This looked a little beyond our expertise and so my students and I drove to Colorado to work with John Hall, to attempt this; this was unsuccessful. Then it occurred to us that, for this purpose, it is much easier to use an external electric field to cause the $Q_1(0)$ transition. Since it is trivial to switch the field on and off we should be able to use the effect as molecular modulation. Such an effect has been predicted by Condon [15] in the early years of spectroscopy; we call this effect the Condon effect and the modulation Condon modulation. More background of this effect and the detail of the experiment are given in Ref. 14.

Technical difficulties (*a*) of inserting the high voltage electrode into the cell and growing a good transparent crystal between the electrode and the wall of the sample cell, and (*b*) of applying high electric field without breakdown, have been overcome by graduate student Karen Kerr. An example of the observed signal is shown in Fig. 3. The use of Condon modulation has improved the sensitivity of our spectroscopy by two orders of magnitude to $\Delta I/I \approx 5 \cdot 10^{-6}$. Now the experiment is much simpler. We use a color center laser as the tunable infrared source which can be stabilized to $\lesssim 0.5$ MHz if necessary. This technique has been used to observe the variation of the $Q_1(0)$ spectral line depending on temperature. An example is shown in Fig. 4. Details of the observation and its interpretation are in Ref. 14. This technique is very versatile and has already been applied in many cases [11].

5. Impurity-induced spectrum

The $J = 1$ ortho-H_2 molecules, which exist in para-H_2 crystals as impurities (typically 0.2%) as a result of incomplete ortho-to-para conversion, have nonzero average quadrapole moment and thus exert a $1/R^4$ quadrupolar electric field on the surrounding para-H_2 molecules. This field at the position of the i-th molecule is expressed as

$$E(\mathrm{R}_i) = Q\nabla \sum_m C_{2m}(\hat{\Omega}) C^*_{2m}(\hat{\Omega}_i)/R_i^3 \ ,$$

where Q is the quadrupole moment of H_2, ∇ is the gradient; $C_{2m}(\hat{\Omega})$ and $C_{2m}(\hat{\Omega}_i)$ are the Racah spherical harmonics for the angular coordinates $\hat{\Omega}$ of the $J = 1$ H_2 and the angular position $\hat{\Omega}_i$ of the i-th molecule, respectively; and R_i is the distance from the $J = 1$ H_2 to the i-th molecule. The magnitude of the electric field is on the order of $E \sim \sqrt{3}Q/R^4 \sim$ $\sim$ 1 MV/cm at the nearest neighbor sites and induces the $Q_1(0)$ transition. Because of the strong field, the induced spectrum has higher integrated intensity than the previous two cases. However, the short-range, randomly localized field destroys the translational symmetry of the crystal and the $\Delta k = 0$ rule is not followed, resulting in a broad spectral line. An

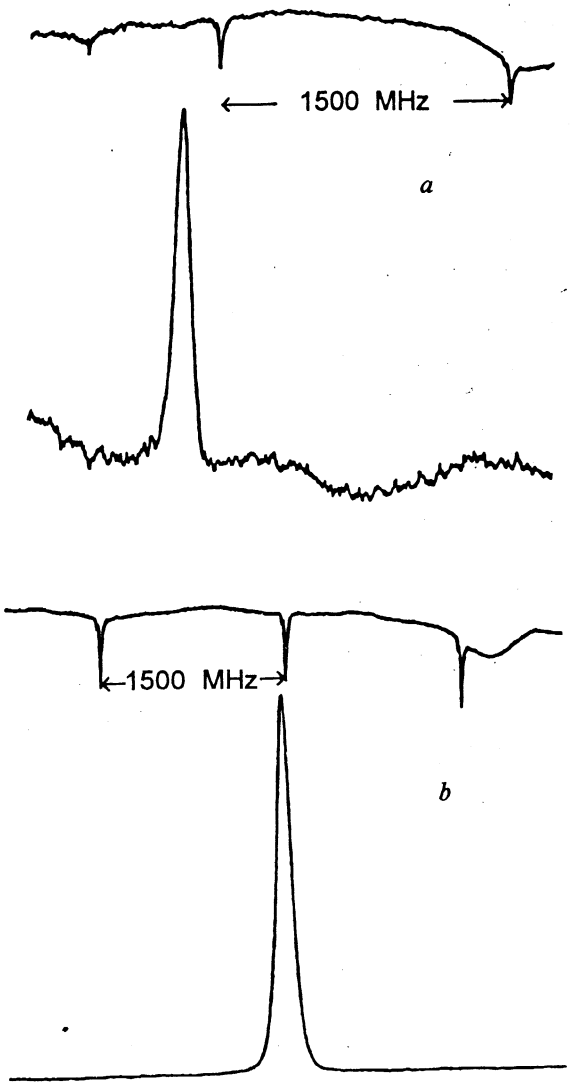

Fig. 3. Observed electric field induced $Q_1(0)$ transition in 99.8% pure para-H_2 crystal. A difference frequency system was used as the radiation source. The wavenumber of the spectral line was measured to be 4149.6918 cm^{-1}. In the upper figure, a dc electric field of 8 kV/cm was applied and videodetection using a chopper was employed. In the lower figure Condon modulation with a 10 kHz sine wave ac field of 6 kV/cm peak to peak was used followed by $2f$ detection. The polarization of the laser field is parallel to the applied field. The signal disappears when they are perpendicular. A sensitivity of $\Delta I/I \approx 5 \cdot 10^{-6}$ was obtained for a time constant of 3 sec.

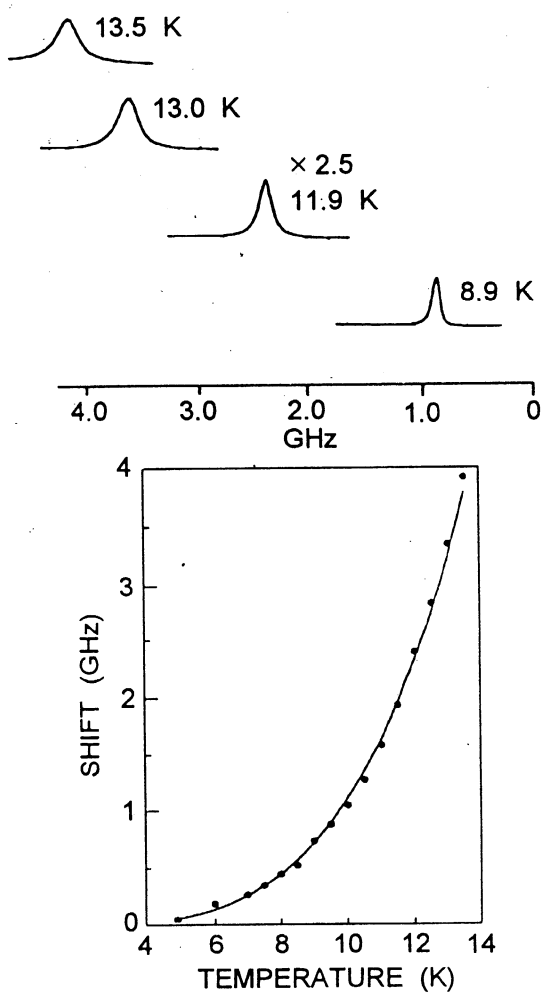

Fig. 4. Temperature variation of the $Q_1(0)$ transition. The spectral frequency blue shifts by ~ 4 GHz as the temperature is varied from 4.2 to 13.5 K. The linewidth increases by a factor of ~ 4. Note that the lineshape changes from near Gaussian shape to almost perfect Lorentzian. For the discussion see Ref. 14.

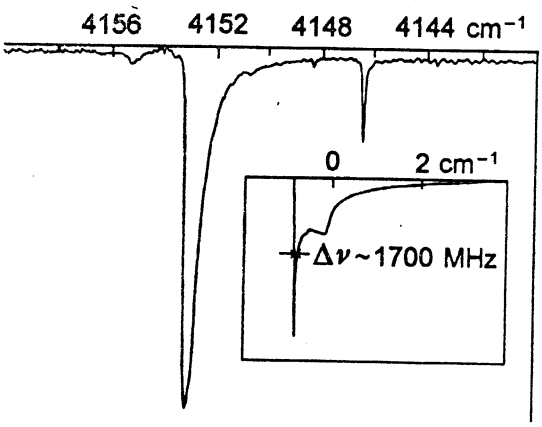

Fig. 5. The broad spectral feature corresponding to the $Q_1(0)$ transition of H_2 induced by the quadrupolar electric field of $J = 1$ H_2. Breakdown of translational symmetry violates the $\Delta k = 0$ rule. Inset shows the vibron energy spectra calculated by Bose and Poll [16]. A BOMEM DA2 Fourier transform spectrometer was used for the observation.

example is shown in Fig. 5. Included in the figure is the theoretical vibron energy spectrum calculated by Bose and Poll [16], which agrees with the observation semiquantitatively.

While the quadrupolar field of the $J = 1$ H_2, when acting on the host $J = 0$ H_2, induces a broad spectrum, it induces a sharp spectrum on impurities such as $J = 0$ D_2 or HD which are embedded randomly in the crystal in small concentration. In this case the vibron is well localized because of the large energy mismatch between the D_2 or HD impurity and the surrounding para-H_2. The resulting $Q_1(0)$ transition of D_2 or HD, however, are accompanied by simultaneous transitions of the $J = 1$ H_2 and show intricate structure which has been a puzzle for us for the last few years [17]. We have now completely understood this structure thanks to a very thorough and persistent effort by graduate student David Weliky and theoretical calculations by Teri Byers [11]. I regard this to be a major progress. When the concentration of D_2 or HD impurities is small, vibrons are well localized on impurity sites and the spectral lines are observed to be extremely sharp ($\Delta\nu \approx 2$ MHz *hwhm*). However, when the concentration of the impurity is increased, every spectral line starts to show a structure that somewhat resembles the structure of vibron bands as shown on the right in Fig. 6. It is likely that this structure is caused by vibron hopping among randomly distributed impurities which produce some Bloch-type state. I believe this phenomenon poses a well-defined interesting theoretical problem.

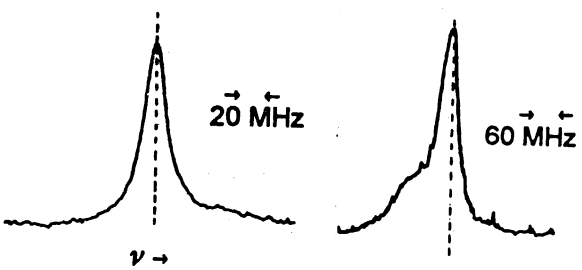

Fig. 6. The sharp spectral line of D_2, induced by the electric field of $J = 1$ H_2. On the left is the spectrum of a sample containing 0.1% $J = 0$ D_2. On the right is the spectrum of a sample containing 0.4% $J = 0$ D_2. The latter shows asymmetric vibron-like line shape due to vibron hopping among randomly localized D_2. Both samples contain 0.2% ortho-H_2 impurity. A color center laser was used for the observation.

6. Charge-induced spectrum [18]

In our attempt to observe behavior of electric charges in the crystal, we ionized solid hydrogen by using accelerated electrons (3 MeV) and γ-ray radiation. After a few years of trial and error we found that the latter method is superior because of its efficiency, its ability to produce uniform ionization, and its ease of operation. High-energy (1.17 and 1.33 MeV) γ-ray ionize H_2 to form H_2^+, initially by Compton scattering. The scattered electrons, having energies of a fraction of MeV, initiate cascades of ionizations. Altogether approximately $1.5 \cdot 10^{17}$ cm^{-3} of ionizations occur in the crystal after one hour of γ-ray irradiation. Such intense ionization would leave the ordinary dielectric materials as rubble of radiation damage, but the extraordinary self-repairing nature of solid hydrogen keeps the crystal still ordered and transparent to radiation.

An example of the charge induced spectrum is shown in Fig. 7. To our surprise, the spectrum is very

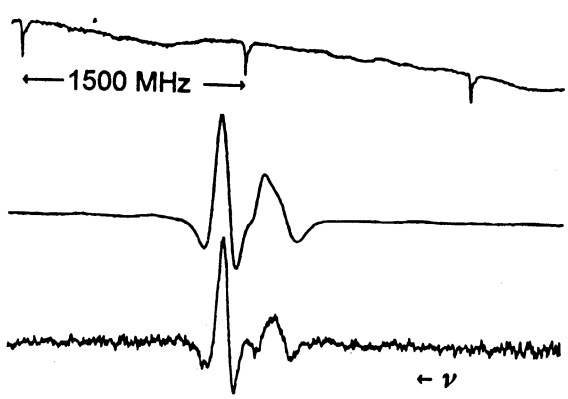

Fig. 7. Simultaneously recorded signals of the γ-ray induced $Q_1(0)$ transition using infrared spectroscopy (middle trace) and stimulated Raman spectroscopy (lower trace). The upper trace gives interference fringe of a spectrum analyzer separated by 1500 MHz. The position and the sharpness of the spectrum demonstrate that the $\Delta k = 0$ rule is well obeyed. The structure similar to that in Fig. 2 is yet to be understood.

sharp and intense, and appears very close in frequency to the position of the Raman (or Condon) spectrum. This clearly shows that the spectrum is induced by the electric field of the charges introduced in the crystal by γ-ray radiolysis and that there exists a well defined vibron Bloch state and the $\Delta k = 0$ selection rule holds. The structure of the line seen in Fig. 7 varies from crystal to crystal and resembles that of the Raman spectrum for high ortho concentrations (Fig. 5); we have not understood it yet. Based on Condon's theory, the intensity of the signal gives estimates of the average charge-induced electric field to be 4–12 kV/cm. One surprising aspect of the charge induced signal is its stability. When the crystal temperature was varied from 4.2 to 13.5 K near the triple point, the frequency of the spectrum was blue shifted by ~ 4 GHz similar to the Condon spectrum discussed earlier. When the temperature was brought back to 4.2 K, the signal came back to the original position with the original intensity. The reproduction of the signal after temperature cycles demonstrates the amazing stability of the charges distributed in the crystal.

We speculate that positive charges are stabilized and localized by the following processes. The H_2^+ ions produced by γ-ray radiolysis immediately react with surrounding H_2 to form H_3^+ through the well known efficient reaction [19]

$$H_2 + H_2^+ \rightarrow H_3^+ + H \ .$$

The H_3^+ thus produced attracts neighboring H_2 and stabilizes in the form of cluster ions $H_3^+(H_2)_n$. An estimate of the number density of the positive charge thus stabilized depends a lot on the fate of negative charges. The electrons ejected due to γ-ray radiolysis cannot reside on H_2 molecules and migrate around in the crystal. Most of them recombine with the positive charges and are neutralized. Some of them may reach the wall of the container and leak into it (the work function of Cu is 4.56 eV). However, some of them may combine with hydrogen atoms, copiously produced by the γ-ray radiolysis [20], and get stabilized in the form of $H^-(H_2)_n$. If we assume the extreme case in which no negative charge is stabilized in the crystal, the observed electric field of ~ 10 kV/cm gives the positive charge density estimate of $\sim 10^{10}\,cm^{-3}$ from Gauss' theorem. On the other hand, if we assume the opposite extreme in which the number densities of the positive and negative charges are equal and the crystal is overall neutral, then we obtain an estimate of $\sim 10^{15}\,cm^{-3}$. We shall attempt to determine the charge density by directly observing spectra of $H_3^+(H_2)_n$ cations. For both extreme cases, the long range Coulomb field covers sufficient domain of the crystal for the vibron Bloch state to exist and the $\Delta k = 0$ rule to hold. More details of this argument are given in Ref. 18.

Acknowledgement

Works summarized in this paper were done in collaboration with T. Momose, D. P. Weliky, T. J. Byers, K. E. Kerr, R. M. Dickson, and Y. Zhan. The research was supported by the Air Force grants #F33615-90C-2035 and #F49620-94-1-0145. It is also partially supported by NSF grant PHY-9321913. I wish to thank M. A. Strzhemechny for critical reading of this paper.

1. I. F. Silvera, *Rev. Mod. Phys.* **52**, 393 (1980).
2. A. R. W. McKellar, *J. Chem. Phys.* **92**, 3261 (1990).
3. L. H. Nosanow, *Phys. Rev.* **146**, 120 (1966).
4. M. C. Cross and D. S. Fisher, *Rev. Mod. Phys.* **57**, 881 (1985).
5. M. Roger, J. H. Hetherington, and J. M. Delrieu, *Rev. Mod. Phys.* **55**, 1 (1983).
6. H. Meyer, *Can. J. Phys.* **65**, 1453 (1987).
7. R. Oyarzun and J. Van Kranendonk, *Can. J. Phys.* **50**, 1494 (1972).
8. J. M. Delrieu and N. S. Sullivan, *Phys. Rev.* **B23**, 3197 (1981).
9. J. Van Kranendonk, *Solid Hydrogen*, Plenum Press, New York (1983).
10. T. Oka, *Annu. Rev. Phys. Chem.* **44**, 299 (1993).
11. D. P. Weliky, T. J. Byers, K. E. Kerr, T. Momose, R. M. Dickson, and T. Oka, *Appl. Phys.* **B59**, 265 (1994) (in press).
12. T. Momose, D.P. Weliky, and T. Oka, *J. Mol. Spectrosc.* **153**, 760 (1992).
13. T. Momose, K. E. Kerr, R. M. Dickson, Y. Zhan, and T. Oka, (Manuscript in preparation).
14. K. E. Kerr, T. Momose, D. P. Weliky, C. M. Gabrys, and T. Oka, *Phys. Rev. Lett.* **72**, 3957 (1994).
15. E. U. Condon, *Phys. Rev.* **41**, 759 (1932).
16. S. K. Bose and J. D. Poll, *Can. J. Phys.* **68**, 159 (1990).
17. M.-C. Chan, L.-W. Xu, C.M. Gabrys, and T. Oka, *J. Chem. Phys.* **95**, 9404 (1991).
18. T. Momose, K. E. Kerr, D. P. Weliky, C. M. Gabrys, R. M. Dickson, and T. Oka, *J. Chem. Phys.* **100**, 7840 (1994).
19. T. Oka, *Rev. Mod. Phys.* **64**, 1141 (1992).
20. T. Miyazaki, S. Kitamura, H. Morikita, and K. Fueki, *J. Phys. Chem.* **96**, 10331 (1992).